Desalination xxx (xxxx) xxx–xxx

Contents lists available at ScienceDirect

Desalination

journal homepage: www.elsevier.com/locate/desal

Osmotically assisted reverse osmosis for high salinity brine treatment

Timothy V. Bartholomew[a,b], Laura Mey[a], Jason T. Arena[b], Nicholas S. Siefert[b], Meagan S. Mauter[a,c,*]

[a] Department of Civil and Environmental Engineering, Carnegie Mellon University, 5000 Forbes Ave., Pittsburgh, PA 15213, USA
[b] National Energy Technology Laboratory, U.S. Department of Energy, 626 Cochrans Mill Rd., P.O. Box 10940, Pittsburgh, PA 15236, USA
[c] Department of Engineering and Public Policy, Carnegie Mellon University, 5000 Forbes Ave., Pittsburgh, PA 15213, USA

ABSTRACT

This work evaluates a novel osmotically assisted reverse osmosis (OARO) process for dewatering high salinity brines using readily available membranes and equipment. While traditional reverse osmosis processes are limited to treating brines with osmotic pressures below the membrane burst pressure, in OARO, the osmotic pressure difference across a membrane is reduced with a permeate side saline sweep. A series of OARO stages can be used to sequentially reduce the concentration of the feed until a traditional RO process can obtain fully desalinated water. This paper develops an OARO model to identify feasible operating conditions for this process and to estimate the water recovery and energy consumption across a range of brine feed concentrations. For a feed of 100–140 g/L sodium chloride, we estimate that the OARO process is capable of a 35–50% water recovery with an energy consumption of 6–19 kWh per m^3 of product water. The results suggest that an OARO dewatering process improves upon the recovery of reverse osmosis for high salinity brines and has a comparable or lower energy consumption than mechanical vapor compression.

1. Introduction

There is growing demand from the oil and gas, electric power, and industrial sectors for processes to desalinate high salinity brines with 50–350 g/L of total dissolved solids (TDS) [1–3]. Current brine dewatering techniques are expensive, energy intensive, or limited to low water recovery. There is an urgent need for new, scalable methods for concentrating brine prior to crystallization or disposal.

Current technologies for brine dewatering include both evaporative and non-evaporative approaches. The most common evaporative technologies include multi-stage flash distillation (MSF), multi-effect distillation (MED), membrane distillation (MD), and mechanical vapor compression (MVC) [4,5]. MSF, MED, and MD processes use thermal energy, commonly steam, which limits the practicality of these processes on field-deployable skids [1,4]. In contrast, the MVC process uses only electricity and is now widely adopted for dewatering high salinity brines in the oil and gas industry [1]. As an evaporative process, the energy consumption of MVC ranges from 11 to 25 kWh per m^3 of produced water, which is significantly greater than the theoretical minimum work of approximately 1–5 kWh per m^3 to dewater a brine with TDS of 35–150 g/L at 50% recovery [6].

By avoiding a phase change, non-evaporative membrane based technologies may reduce the energy intensity of desalination and brine dewatering processes. Reverse osmosis (RO), forward osmosis (FO), and pressure assisted forward osmosis (PAFO) offer several pathways for brine dewatering across a semi-permeable membrane [7–10]. Fig. 1A presents the set driving and retarding forces in membrane-based separation processes where positive water flux is defined as flow against the osmotic pressure difference from the feed side (f) to the permeate side (p) of the membrane. A positive hydraulic pressure difference ($P_f - P_p$, ΔP) drives water transport, while a negative ΔP retards water transport. In contrast, a positive osmotic pressure difference ($\pi_f - \pi_p$, $\Delta\pi$) retards water transport, while a negative $\Delta\pi$ drives water transport.

In RO, a positive hydraulic pressure difference ($+\Delta P$) drives water transport against the retarding force of a positive osmotic pressure difference ($+\Delta\pi$). In FO, there is a negligible hydraulic pressure difference ($\Delta P \approx 0$) and a highly concentrated draw solution establishes a negative osmotic pressure difference ($-\Delta\pi$) to drive water flux from the feed to the draw. In PAFO, a positive hydraulic pressure gradient is used to augment the negative osmotic gradient of FO ($+\Delta P$, $-\Delta\pi$). While not a separation process, pressure retarded osmosis (PRO) processes utilize the hydraulic pressure as a retarding force ($-\Delta P$) and the osmotic pressure as the driving force ($-\Delta\pi$). Of these membrane processes, only RO directly dewaters brines. FO and PAFO require a second process, most commonly a RO or thermal draw solute regenera-

* Corresponding author at: Department of Civil and Environmental Engineering, Carnegie Mellon University, 5000 Forbes Ave., Pittsburgh, PA 15213, USA.
E-mail address: mauter@cmu.edu (M.S. Mauter).

http://dx.doi.org/10.1016/j.desal.2017.04.012
Received 8 December 2016; Received in revised form 17 April 2017; Accepted 17 April 2017

Nomenclature

Treatment technology

FO	forward osmosis
MD	membrane distillation
MED	multi-effect distillation
MSF	multi-stage flash distillation
MVC	mechanical vapor compression
OARO	osmotically assisted reverse osmosis
PAFO	pressure assisted forward osmosis
PRO	pressure retarded osmosis
RO	reverse osmosis

Variables

P	hydraulic pressure
ΔP	hydraulic pressure difference across the membrane
π	osmotic pressure
Δπ	osmotic pressure difference across the membrane
A	pure water permeability coefficient
J_w	water flux
i	number of dissociating ions
φ	osmotic coefficient
C	solute concentration
R	gas constant
T	temperature
k	feed mass transfer coefficient
K	solute resistivity for diffusion in the porous support

Subscripts

f	feed side
p	permeate side
s	sweep side
b	bulk
m	membrane surface

tion step, to produce a pure water permeate.

While non-evaporative membrane-based processes more closely approach the thermodynamic minimum of separation for seawater desalination, they are limited in their effectiveness for treating high salinity brines [11]. RO water recovery is limited for high salinity brines (> 50 g/L) because the hydraulic pressure cannot exceed the membrane burst pressure (membrane dependent, but typically about 70–80 bar) [7]. While ongoing research is focused on increasing this burst pressure, operating at ultra-high pressures may lead to severe compression of the polymer active layer and greater irreversible fouling. FO processes simply perform a salt exchange across a membrane, and thus do not dewater brines in the traditional sense without a second membrane, thermal, or solvent induced separations step.

Osmotically assisted reverse osmosis (OARO) is a non-evaporative, membrane-based process for high recovery, energy efficient desalination of high salinity brines [3,12–14]. OARO, like RO, uses hydraulic pressure to transport water across a semi-permeable membrane against the osmotic pressure difference between the feed and permeate (+ ΔP, − Δπ). Unlike RO, where the permeate TDS approaches zero, OARO has a permeate-side saline sweep to reduce the osmotic pressure difference across the membrane. This modification enables water transport even when the osmotic pressure of the feed exceeds the burst pressure of the membrane. Therefore, OARO expands the maximum TDS from which water can be recovered from a hydraulic pressure driven membrane processes (Fig. 1B). When multiple OARO stages are linked in series, this process enables the recovery of freshwater from high salinity brines.

The present work explores the theoretical limits of OARO processes and quantifies key performance metrics. We develop a discrete model that includes concentration polarization effects, and we apply this model to estimate the water recovery and energy consumption of the OARO process. We also explore the decision space of the OARO process by varying inlet feed and sweep concentrations, the feed pressure, the number of OARO stages, and the membrane area. Additionally, we compare the performance of OARO to other electricity driven desalination technologies, MVC and RO. Finally, we discuss the limitations of our model and identify the critical research steps necessary to fully assess the technical and economic feasibility of the OARO process.

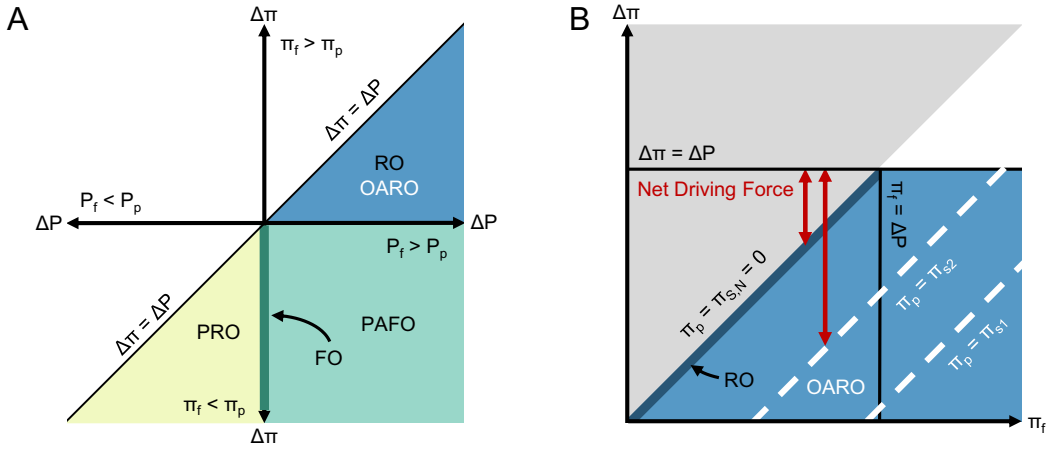

Fig. 1. A) Driving and retarding forces for reverse osmosis (RO), osmotically assisted reverse osmosis (OARO), forward osmosis (FO), pressure assisted forward osmosis (PAFO), and pressure retarded osmosis (PRO) membrane processes. We define the feed side (f) and permeate side (p) of the processes by the direction of the water flux (feed to permeate). Hydraulic pressure difference ($P_f - P_p$, ΔP) is a driving force when positive and is a retarding force when negative. Osmotic pressure difference ($\pi_f - \pi_p$, Δπ) is a retarding force when positive and is a driving force when negative. The white region is where the driving force is smaller than the retarding force, thereby changing the direction of water transport and inverting the definition of the feed side and permeate side. B) RO (dark blue line, $\pi_p = 0$) and OARO process region (blue) for two potential sweep concentrations (white dotted lines, $\pi_p = \pi_{s,1}$, $\pi_p = \pi_{s,2}$) at a constant applied hydraulic pressure difference (ΔP). The net driving force (ΔP − Δπ) of OARO is greater than the net driving force of RO with the same π_f. The grey region represents the infeasible case of π_p being negative. (For interpretation of the references to color in this figure legend, the reader is referred to the web version of this article.)

2. Multi-staged osmotically assisted reverse osmosis process for water recovery

OARO is a novel process for realizing moderate water recoveries from high salinity brines at ambient temperatures via a membrane-based separation process. Fig. 2 presents a schematic diagram of the proposed OARO process requiring multiple stages to produce desalinated water. Here, a high salinity feed is fed into an OARO module at a high hydraulic pressure. On the permeate-side of the module, a low-pressure sweep with a lower salinity flows counter-current to the feed. The high-pressure feed and low-pressure sweep establishes a hydraulic pressure difference that is greater than the osmotic pressure difference across the membrane. The resulting water flux concentrates the feed and dilutes the sweep. The concentrated feed is the reject from the OARO process and may be crystallized or otherwise disposed.

If the diluted sweep concentration is relatively high and the target recovery is not achievable via RO, then the diluted sweep can be pressurized and fed into a second OARO module. Since the diluted sweep has a lower concentration than the original feed, an equivalent permeate volume can be realized with a lower sweep concentration. This second OARO module re-concentrates the diluted first sweep and dilutes the second sweep. The re-concentrated first sweep can be reused as the sweep inlet for the first OARO module and the diluted second sweep may require another OARO stage. The sweep concentrations successively decrease over a series of OARO stages until the sweep concentration is sufficiently low for RO. Ultimately, the OARO process will involve a feed inlet, a concentrated waste outlet, closed cycles of saline sweeps, and a product water outlet.

2.1. Energy consumption of the OARO process

The primary energy demand of the OARO process is the electricity required to power the pumps to pressurize the feed. A pressure exchanger, represented as a box linking the feed and the permeate streams in Fig. 2, lowers the energy demand by transferring energy from the high pressure waste stream to the low pressure feed before the feed is pumped to the designed pressure [7]. In OARO, not only can the pressure exchanger be used for the feed, it can also be used for each sweep cycle, as shown in Fig. 2. An effective use of multiple pressure exchangers will lower the energy consumption of the OARO process.

2.2. OARO water flux and concentration polarization

Water flux in OARO processes depends upon the hydraulic and osmotic pressure difference across the membrane (Eq. (1)).

$$J_w = A[(P_f - P_s) - (\pi_{f,m} - \pi_{s,m})] \quad (1)$$

here, J_w is the water flux from the feed to the sweep, A is the pure water permeability coefficient, P_f and P_s are the hydraulic pressures for the feed and sweep, and $\pi_{f,m}$ and $\pi_{s,m}$ are the osmotic pressure at the membrane surface for the feed and sweep. The osmotic pressure of a solution can be estimated as a function of solute concentration (Eq. (2)).

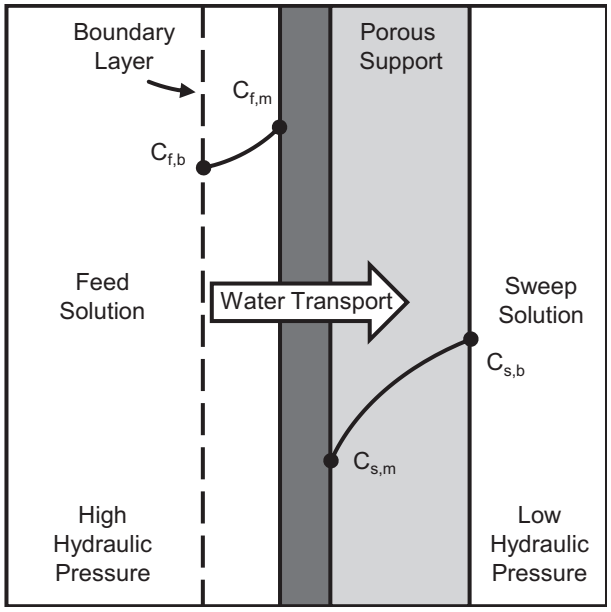

Fig. 3. Schematic diagram of an OARO module and the effects of concentration polarization on the solute concentration at the membrane surface (C∗,m) relative to the bulk concentration (C∗,m) of the feed (f) and sweep (s).

$$\pi(C) = i\phi CRT \quad (2)$$

here, i is the number of dissociating ions, ϕ is the osmotic coefficient, C is the solute concentration, R is the gas constant, and T is the temperature. Oftentimes, the solution is assumed to be ideal, ϕ = 1. However, solutions with high solute concentrations deviate significantly from ideal behavior. To account for non-ideal behavior, we model the osmotic coefficient as a function of solute concentration based on experimental results.

The osmotic pressure at the membrane surface is determined by adjusting the bulk solute concentration for concentration polarization effects [15]. In concentration polarization, water flux increases solute concentration at the membrane on the feed side and decreases solute concentration at the membrane on the sweep side relative to the bulk concentration, as shown in Fig. 3. The solute concentration at the membrane surface for the feed and sweep can be calculated from Eqs. (3) and (4) [16].

$$C_{f,m} = C_{f,b} \exp\left(\frac{J_w}{k}\right) \quad (3)$$

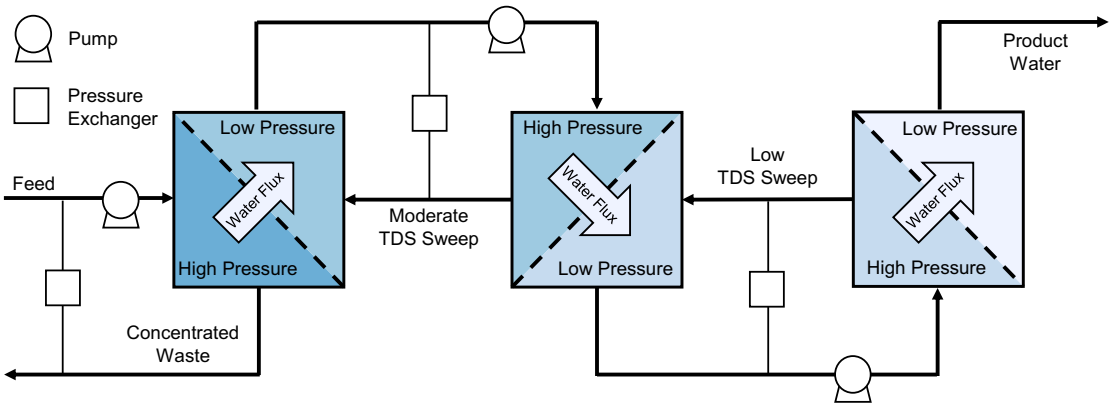

Fig. 2. Process diagram of the OARO process. The first two stages are OARO, while the final stage is RO.

$$C_{s,m} = C_{s,b}\exp(-J_w K) \quad (4)$$

where, $C_{f,m}$ and $C_{s,m}$ are the solute concentrations at the membrane surface for the feed and sweep, $C_{f,b}$ and $C_{s,b}$ are the respective bulk solute concentrations of the feed and sweep, k is the feed mass transfer coefficient, and K is the solute resistivity for diffusion in the sweep side porous support; refer to McCutcheon and Elimelech for further direction in determining these parameters [16].

3. Methods

3.1. Discrete element model for the OARO module

We model the OARO module as a flat plate with counter-current flow. The model uses a discrete element approach and an iterative method to solve the implicit calculations. Additional details on the mass balance equations and solution methods are provided in SI Section 2. The model input variables for a single OARO module include: the module dimensions, and inlet flowrates, concentrations, and hydraulic pressures for the feed and sweep. The model output variables for a single OARO module include: water recovery, and outlet flowrates, concentrations, and hydraulic pressures of the feed and sweep. For simplicity, we assume that the solute for the feed and sweep is sodium chloride, though any solute with low reverse flux, high osmotic pressure, and high diffusivity could be used [17]. We source membrane specific parameters from literature and use regressions of literature sources and databases to determine the concentration dependent solution properties: osmotic coefficient, diffusivity, and density [18–20].

3.1.1. Salt rejection

The amount of salt flux will vary for each OARO module and will lead to salt accumulation or depletion within the sweep cycles. We assume there is no salt flux (100% salt rejection) to simplify the model and assess steady state operation. We consider salt flux and assess the expected salt rejection in SI Section 5.

3.1.2. Transitional flow regime

We assume a Reynolds number of 1000 for the feed and sweep flow. This transitional flow regime is typical of RO and FO processes in which spacers are utilized to promote mixing [21–24]. The effect of different spacer shapes is outside the scope of this work.

3.1.3. Pressure drop

Pressure drop is dependent on: module design, spacers, flow regime, and membrane roughness. We assume a 5 kPa pressure drop per meter of membrane length, which aligns with a combination of previous modeling and experimental work, as well as a friction based analytical calculation [25,26]. The sensitivity of the pressure drop on the performance of the OARO process is presented in SI Section 6.

3.2. Determining the number of modules and estimating the energy consumption

The OARO process is a system of modules that successively decreases the sweep concentration until a RO unit can be used to dewater a brine without exceeding the burst pressure of the membrane. To model this process, we require the OARO process to operate at steady state such that the permeate volume is equivalent across the multiple modules. Therefore, after the first OARO module is specified, successive OARO module design is deterministic.

We determine the operating parameters for successive modules by fixing design variables and adjusting the sweep concentration. We hold the module dimensions, inlet pressure, and sweep flow constant across all stages. We then adjust the sweep concentration for each OARO module to obtain the same permeate volume as the first module. Eventually, the last module will require a sweep TDS of zero, at which point a RO module is specified. Since there is no sweep for the RO module, we adjust the feed pressure to obtain the same permeate volume as the first module. Once the entire OARO process is specified, we can determine the total number of modules and estimate the energy consumption of the high-pressure pumps. In calculating the energy consumption, we assume the pumps have an 80% isentropic efficiency and the pressure exchangers are 96% efficient [7].

Table 1
User specified variables for the OARO base-case scenario.

Parameter	Symbol	Value	Units
Module length	L	10	m
Module width	W	1	m
Module height	H	1	mm
Feed inlet flowrate	Q_f	1.0E − 05	m^3/s
Sweep inlet flowrate	Q_s	5.0E − 06	m^3/s
Feed inlet pressure	P_f	65	bar
Feed TDS	C_f	125	g/L
Sweep inlet pressure	P_s	2	bar
First sweep TDS	C_s	175	g/L

3.3. Base case

We define a base-case scenario to provide a thorough example of the OARO process and establish a basis from which to compare other operating conditions. Our base case achieves the goal of > 30% freshwater recovery for a 125 g/L sodium chloride brine. Table 1 provides the user specified variables of the base-case scenario. We use a common RO operating pressure of 65 bar, which is below the assumed membrane burst pressure of 70 bar. The module dimensions are arbitrarily chosen in this study. We assume the sweep inlet flowrate is half of the feed inlet flowrate. We assume the membrane specific parameters are 1.0×10^{-12} m/(s-Pa) for the water permeability coefficient and 1000 μm for the structural parameter, which is representative of a commercial, asymmetric, cellulose triacetate membrane [19]. We assume a temperature of 298 K for both the feed and sweep solutions.

4. Results and discussion

The OARO process expands the use of membrane-based separation processes for high salinity brine dewatering. OARO can increase water recovery at hydraulic pressures below the membrane burst pressure by utilizing a saline sweep to reduce the osmotic pressure difference across the membrane. The sweep concentration is reduced in successive stages until the diluted sweep can be effectively treated using a traditional RO process. The OARO process has several key design considerations, such as: freshwater recovery, inlet feed and sweep concentration, hydraulic pressure of the feed, number of stages, and membrane area. We assess these design variables by systematically varying the parameters around the base-case scenario established in Table 1.

4.1. Systematic analysis of OARO performance as a function of key design parameters

The purpose of the OARO process is to obtain higher water recoveries than RO by utilizing saline sweeps to reduce the osmotic pressure difference across the membrane. Fig. 4A provides the simulated recovery for an OARO module with the base case module dimensions and a feed pressure of 65 bar across a range of inlet feed and sweep concentrations. The sweep with zero TDS has a recovery of 54% for a feed TDS of 35 g/L, which matches the expected performance of RO processes. As the feed concentration increases, the recovery rate from the RO process drops sharply to only 4% for a feed TDS of 75 g/L. This sharp decrease in recovery at higher feed concentrations demon-

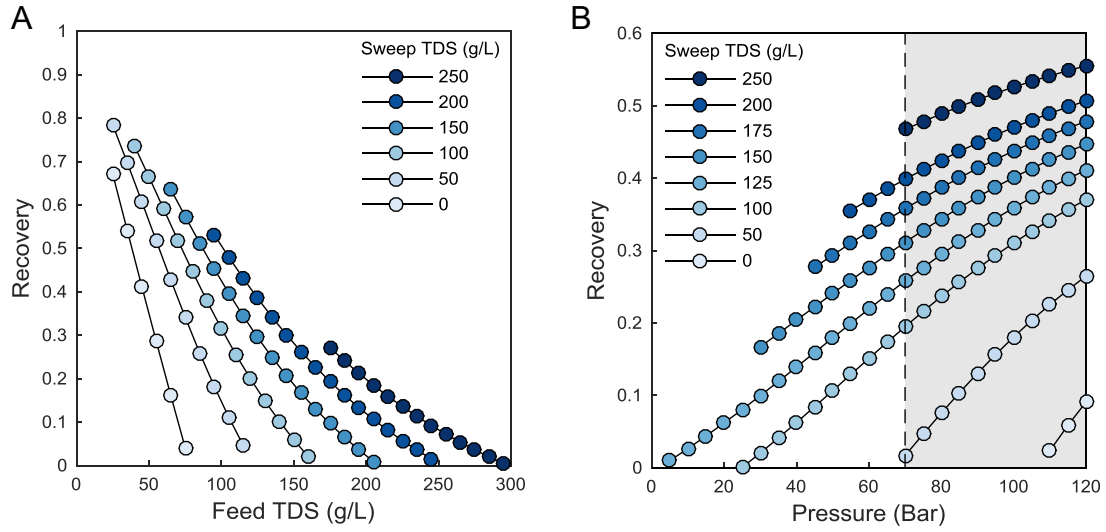

Fig. 4. OARO module recovery with base case module dimensions. A) OARO module recovery for a constant feed pressure of 65 bar and variable feed and sweep concentration. Cases with high sweep concentration and low feed concentrations operate as PAFO and are omitted from this graph. B) OARO module recovery for a feed with a TDS of 125 g/L sodium chloride and variable feed pressure and sweep concentration. The shaded region represents infeasible operating pressures based on the assumed membrane burst pressure of 70 bar (dotted line). Cases with high sweep concentrations and low feed pressure operate as PAFO and are omitted from this graph.

strates the value of the OARO process for enhancing recovery of high salinity brines. Using saline sweeps increases the recovery for a given feed concentration, and recoveries > 30% are obtained for feed TDS up to 145 g/L with sweep TDS up to 200 g/L.

Fig. 4B provides the simulated recovery for an OARO module with an inlet feed TDS of 125 g/L across a range of feed pressures and sweep inlet concentrations. For this high salinity feed, RO processes (sweep TDS of 0 g/L) are not capable of recovering any freshwater using membranes with a burst pressure of 70 bar. Therefore, it is necessary to use a saline sweep to obtain operating conditions with higher recoveries and feasible operating pressures. Recoveries above 30% at feasible operating pressures occur only for sweep TDS above 150 g/L. In these instances, the inlet sweep TDS is greater than the inlet feed TDS of 125 g/L. However, the feed concentration is greater than the sweep concentration along the membrane because the module operates in counter-current flow. SI Section 4 provides a detailed description of the modeled concentration profile along the OARO module for the base-case scenario.

The OARO process has a set of physical, process, and operator imposed constraints that define a window of feasible OARO operating conditions. As discussed above, the feed pressure must be below the membrane burst pressure and the concentration of the sweep outlet must be less than that of the feed inlet to realize a series of successively decreasing sweep concentrations. This second constraint is violated at low feed concentrations and high sweep concentrations for some set of feed pressures (Fig. 4A). It is also violated at low feed pressures and high sweep concentrations for some set of feed concentrations (Fig. 4B). In both cases, the water permeate volume is not sufficient to dilute the sweep below the feed inlet concentration, causing the module to operate in a PAFO regime (Fig. 1). Fig. 4 plots only OARO processes, and excludes the PAFO conditions.

In addition to the above physical and process constraints, a minimum target recovery is typically set to achieve water treatment goals. With these three constraints, a defined range for feasible OARO operation can be determined. Given a feed TDS of 125 g/L sodium chloride, minimum recovery of 30%, base-case module dimensions, and membrane burst pressure of 70 bar, the range of feasible inlet sweep TDS is 150–250 g/L and the maximum recovery is ~47%. For much higher feed TDS, the solubility of the solute may be an upper limit of sweep TDS, which for sodium chloride is 357 g/L at ambient temperatures [27].

While a high sweep concentration in the first module enhances water recovery, it also has a profound effect on the multi-module configuration and energy consumption of the process. Here, the multi-module configuration is determined from the first OARO module by requiring successive modules to operate at steady state and assuming all

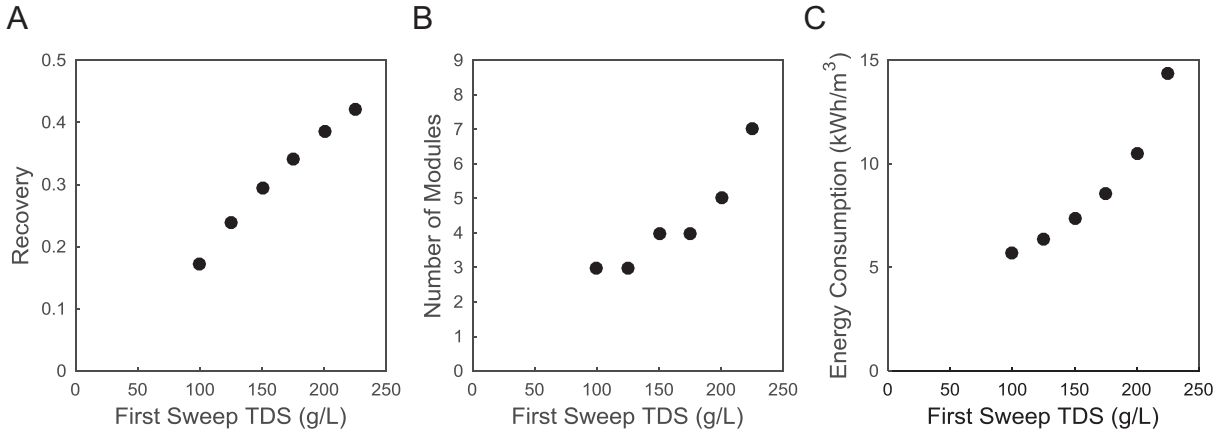

Fig. 5. Recovery (A), number of modules (B), and energy consumption (C) as a function of first inlet sweep concentration for the base-case module dimensions, feed pressure of 65 bar, and inlet feed TDS of 125 g/L sodium chloride.

module and operating variables are constant, except for the sweep concentration, as described in Section 4. Once the entire OARO process is specified, we estimate the energy consumption of the high-pressure pumps. Fig. 5 provides the freshwater recovery, number of modules, and energy consumption of the OARO process with the base case module dimensions, feed inlet pressure of 65 bar, and a feed TDS of 125 g/L sodium chloride.

As the first sweep TDS ranges from 100 to 225 g/L, the recovery, the number of modules, and the energy consumption increases from 17 to 42%, 3 to 7 modules, and 5.7 to 14 kWh per m^3 of produced water, respectively (Fig. 5). Freshwater recovery increases because a higher sweep concentration decreases the osmotic pressure difference across the membrane and increases water flux. The number of modules increases because a higher first sweep concentration directly increases the concentration of the first diluted sweep and requires additional stages to lower the concentration to the point at which an RO module can be used. The energy consumption increases with a higher first sweep concentration for two reasons. First, an increase in the number of modules increases the mechanical energy loss for the system from the pressure drop along the additional module and inefficiencies of the additional high pressure pump and pressure exchanger. Second, in instances where the number of modules stays constant, a higher first sweep concentration will result in a higher diluted sweep concentration into the RO module. Recovering freshwater will thus require higher RO operating pressures and increased energy consumption. The trade-offs associated with the first sweep concentration on recovery, number of modules, and energy consumption will be key design considerations. While higher freshwater recovery will be beneficial, increasing the number of modules and energy consumption will also increase the capital and operating costs of the OARO system.

In addition to the process configurations, the type and dimensions of the module will influence the OARO process. In principle, the OARO module could adopt any configuration with a permeate side sweep. An ideal OARO module configuration will have counter-current feed and sweep flow, relatively high turbulence, and relatively low pressure drop. Counter-current feed and sweep flow minimizes the osmotic pressure difference across the membrane. As in RO, a relatively high turbulence is preferred to reduce concentration polarization effects and a relatively low hydraulic pressure drop across the module will increase water flux and pressure recovery. However, turbulence and pressure drop increase together, so the trade-off between increasing the turbulence and lowering the pressure drop will be a key design consideration. Another design consideration is the membrane area for each module. While increasing membrane area will increase the freshwater recovery, it also increases the pressure drop, salt permeate, and capital and operating costs of the OARO module. Varying the membrane area adds another dimension to the OARO operating decision space, and this dimension is investigated further in Section 4.3 when the recovery of the process is set.

In addition to considering the feed and sweep concentration, feed pressure, recovery, the number of modules, energy consumption, and module dimensions, the OARO process is dependent upon membrane properties. An ideal OARO membrane would have high water permeability, high water selectivity, high membrane burst pressure, and a low structural parameter. RO membranes are designed for only three of the four ideal properties: high water permeability, high water selectivity, and high membrane burst pressure [28]. RO membrane design has not prioritized reducing the structural parameter of the membrane support layer because RO does not experience permeate-side concentration polarization. In contrast, FO membranes are designed with low structural parameters, but they are not typically designed for high membrane burst pressures [28]. Ultimately, ideal OARO membranes most closely resemble ideal PRO and PAFO membranes, with high membrane burst pressures and low structural parameters [29,30]. Thus, we base the membrane properties on a commercially available cellulose triacetate asymmetric membrane commonly used in FO, PRO, and PAFO experiments [19].

This section has detailed the general operating conditions for OARO processes over the range of feedwater salinities and recovery rates attractive for brine treatment associated with common industrial processes. In the subsequent sections, we detail the process variables and separation performance for the base case established in Table 1, providing detailed information about the process configuration, the concentration of each sweep, and the process performance as a function of membrane area and feed pressure.

4.2. Detailed process conditions in base case

The base case requires four modules, as shown in Fig. 6, and has an average water flux of 1.3 L/(m^2 h), a recovery of 34%, and energy consumption of 8.6 kWh per m^3 of produced water. Fig. 7 provides the corresponding concentration profiles of the feed and sweep cycles. The three OARO modules decrease the sweep TDS to 37 g/L (stream 8 in Figs. 5 and 4), which is sufficiently low for the final RO module to achieve the same permeate volume as the upstream OARO modules. The detailed process configuration and variables of the base case demonstrates the OARO treatment process can treat a high salinity feed (125 g/L TDS) through successively decreasing the concentration of the sweeps, but that the flux for this OARO example lies significantly below the flux that is typical for RO.

4.3. Effect of membrane area on energy consumption for a set recovery

To evaluate the effect of membrane area on OARO process performance, we set the freshwater recovery at 35 and 40% and assess how increasing the module membrane area (10 m^2 in the base-case scenario) influences the energy consumption of the OARO process. We adjust the first sweep inlet concentration to maintain a constant

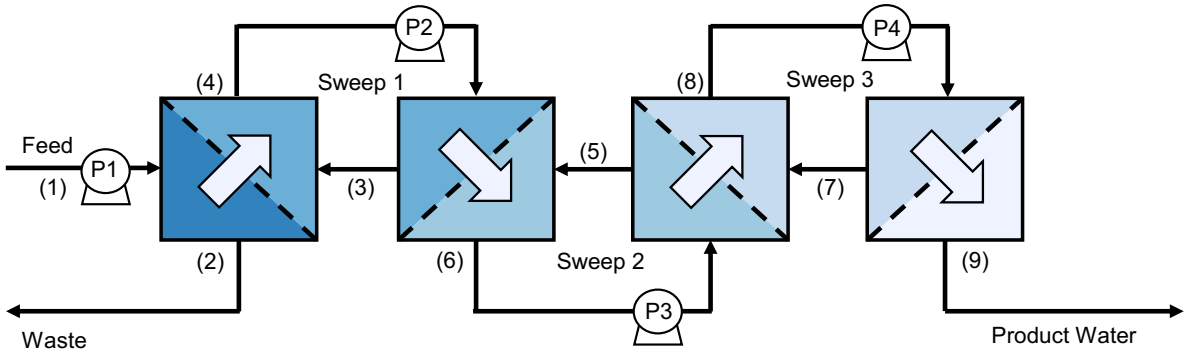

Fig. 6. The multi-module OARO process for the base-case scenario. The first three modules are OARO and the last module is RO. The streams are numbered (1)–(9). There are four pumps (P1–P4) and four pressure exchangers for the feed and sweep cycles (not shown).

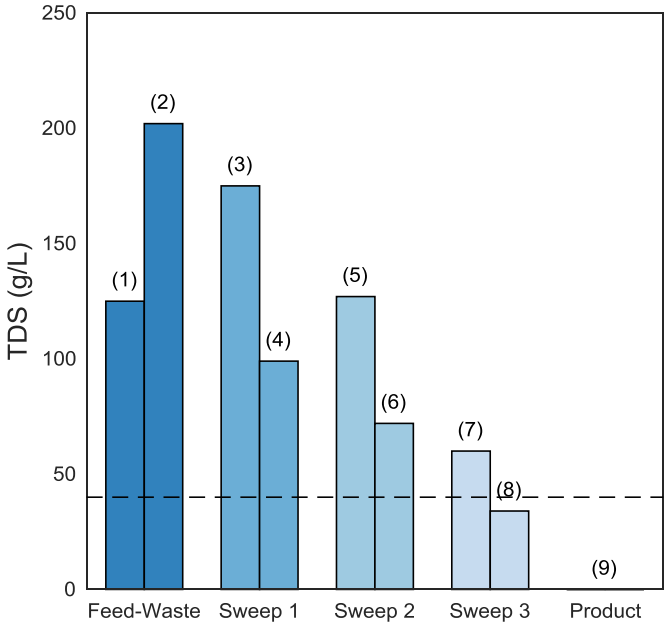

Fig. 7. Concentration profile of the feed and sweep cycles for the base case. The streams (1)–(9) are labeled in Fig. 6. The dotted line represents the typical TDS upper limit (40 g/L) of economically viable reverse osmosis.

recovery for the variable membrane area per module. Increasing the membrane area per module from 9 to 13 m^2 decreases the first stage sweep TDS from 185 to 165 g/L and 215 to 190 g/L, the number of modules from 5 to 4 and 7 to 5, and energy consumption from 9.7 to 7.8 and 14.4 to 9.3 kWh per m^3 of produced water for a recovery of 35 and 40%, respectively (Fig. 8). As membrane area increases, the water flux can be lower to obtain the same desired recovery, thereby allowing a lower first sweep concentration. As discussed previously, a lower first sweep concentration results in either a fewer number of modules or a lower concentration of the diluted sweep into the final RO module. Ultimately, fewer number of modules or a lower operating pressure requirement on the RO unit decreases energy consumption.

Although larger membrane area per module decreases energy consumption, continued increases in membrane area are limited economically. Larger membrane areas will have greater capital and operating costs so the trade-off between the marginal performance improvement with increased cost will be a critical design consideration. In instances where a small increase in membrane area per module decreases the number of modules, the total membrane area of the OARO process decreased. For example, when the area per module increased from 9 to 10 m^2 for a 35% recovery, the total membrane area decreased from 45 m^2 (5 modules at 9 m^2 each) to 40 m^2 (4 modules at 10 m^2 each). In these cases, not only did increasing the membrane area per module decrease the energy consumption but it also decreased the total amount of membrane area and likely the associated membrane costs. This finding suggests that for a given recovery it is better to have fewer large OARO modules rather than more numerous small modules to decrease energy consumption and membrane costs.

4.4. Effect of hydraulic pressure on energy consumption for a set recovery

We assess the effect of feed pressure on OARO energy consumption for a set freshwater recoveries of 35 and 40%. We maintain a constant recovery for the variable feed pressure by adjusting the first sweep concentration. Increasing the feed pressure from 55 to 75 bar decreases the first sweep TDS from 195 to 160 g/L and 220 to 190 g/L, the number of modules from 6 to 3 and 8 to 4, and energy consumption from 11.1 to 7.8 and 14.7 to 9.6 kWh per m^3 of produced water for a recovery of 35 and 40%, respectively (Fig. 9). The feed pressure relationship to the first sweep concentration, number of modules, and energy consumption is similar to the membrane area per module for the same reasons. Feed pressure increases the driving force for water flux, thereby allowing a lower first sweep concentration to obtain the target recovery. The lower first sweep concentration results in lower energy consumption through either fewer modules or a lower pressure demand in the final RO module. While higher feed pressures decrease the number of modules and energy consumption, further increases in feed pressure are physically limited by the membrane burst pressure.

4.5. Comparison of OARO energy consumption to other brine treatment processes

The energy consumption is a key metric for assessing the effectiveness and economic feasibility of the OARO process relative to state of the art evaporative processes, such as MVC. Fig. 10 provides literature reported energy consumption values for RO, MVC, and our OARO simulations at a feed pressure of 65 bar and a membrane area per module of 10 and 20 m^2 for recoveries of 35 and 50%, respectively. RO energy consumption ranges from 1 to 2 kWh per m^3 of produced water for brackish (~5 g/L TDS) and seawater (35 g/L TDS) at a 50% recovery [7]. MVC energy consumption ranges from 11 to 25 kWh per m^3 of produced water for seawater (35 g/L TDS) to high salinity brines (150 g/L TDS) at recoveries of 35 to 50% [1,6,31]. The OARO energy consumption is estimated as 2.9 to 3.7 kWh per m^3 of produced water for feed TDS of 60 g/L at 35 and 50% recovery, respectively. At a higher feed TDS of 140 g/L, these values increase to 12.4 and 19.3 kWh per m^3 of produced water for recoveries of 35 and 50%, respectively.

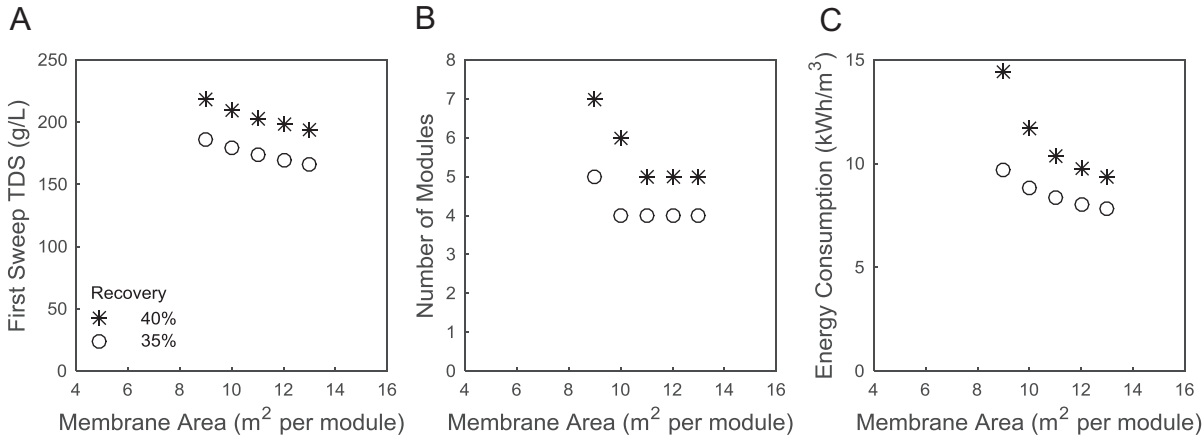

Fig. 8. First sweep concentration (A), number of modules (B), and energy consumption (C) versus membrane area for set recoveries of 35% and 40% (circle and asterisk, respectively). The inlet feed TDS is 125 g/L and feed pressure is 65 bar.

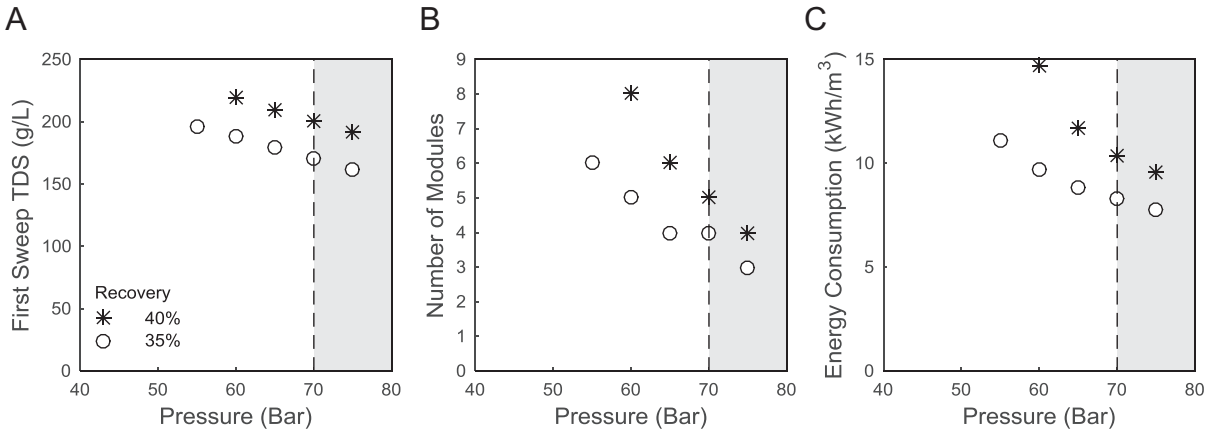

Fig. 9. First sweep concentration (A), number of modules (B), and energy consumption (C) versus feed pressure for set recoveries of 35% and 40% (circle and asterisk, respectively). The inlet feed TDS is 125 g/L sodium chloride and membrane area per module is 10 m^2. The shaded region represents infeasible operating pressures based on our assumed membrane burst pressure of 70 bar (dotted line).

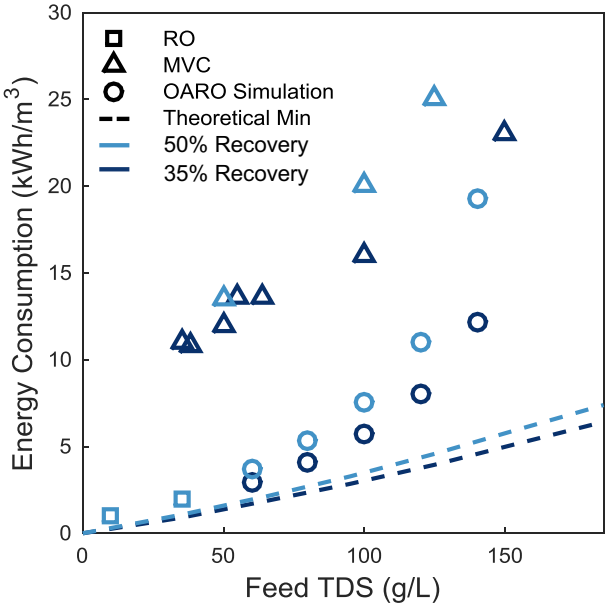

Fig. 10. Energy consumption of RO, MVC, OARO processes and theoretical minimum work with respect to feed concentration and recovery (35% dark blue, 50% light blue). The RO energy consumption is for the desalination of brackish and seawater at a recovery of 50% [7]. The MVC energy consumption spans seawater and higher salinity brines from the oil and gas industry at recoveries of 35–50% [1,6,31]. The OARO simulation uses a feed pressure of 65 bar and a membrane area per module of 10 and 20 m^2 for a recovery of 35 and 50%, respectively. The theoretical minimum work is based on the difference in Gibbs free energy from the inlet feed and outlet products [3]. (For interpretation of the references to color in this figure legend, the reader is referred to the web version of this article.)

These estimates of OARO energy consumption account for losses associated with pressure drop across the module, losses in the pressure exchangers, and the isentropic efficiency of the high pressure pump. We do not account for some inefficiencies in actual system operation, including membrane fouling and incomplete utilization of membrane area. Fig. 10 also presents the theoretical minimum work to dewater the brines, which was calculated as the difference between Gibbs free energy of the inlet feed and the two products (freshwater and concentrated brine) [3]. The Electrolyte NRTL method in AspenPlus is used to determine the Gibbs free energy of the solutions. The dewatering efficiency, defined as the ratio of the minimum theoretical work to the energy consumption, ranges from 30 to 55% for the membrane processes (RO and OARO) and 10–20% for MVC.

As anticipated, the energy consumption of treatment processes increases significantly with increasing feed concentration and freshwater recovery. For all investigated salinities, the membrane-based processes (RO and OARO) have lower energy consumption than MVC. However, MVC can obtain recoveries as high as 90% for brines, which is well above the OARO recoveries from the base case examined in this study [32]. While it is possible to increase the recovery of the OARO process by increasing the total membrane area, the sweep concentrations, and number of modules, these changes would increase the energy consumption and the costs of the OARO process.

4.6. OARO model limitations

This work presents a first order model to estimate key performance metrics of the OARO process. Though the model estimates reasonable recovery rates and energy consumption, there are several other factors including capital costs and pretreatment requirements that will contribute to determining the technical and economic viability of OARO process.

This work does not assess the economics of the OARO process. Without an economic analysis, we cannot determine whether our base case module assumptions and results are feasible. We recognize that many of the critical design variables, such as the membrane area and the number of modules, are solely constrained by costs. In general, the OARO process is expected to have high capital costs due to using multiple membrane modules, high pressure pumps, and pressure exchangers. While multiple modules suggest a high total membrane area, it is expected that the bulk of the capital costs will stem from the physical modules, pumps, and pressure exchangers. This realization suggests that a cost optimal OARO process will likely have a small number of stages, e.g. 2 to 3 large modules. While the maintenance of the membrane and equipment contribute to the operating costs, it is expected that the energy consumption will dominate.

In addition, this work does not address pretreatment processes that are essential for reducing membrane fouling. Pretreatment is especially pertinent for high salinity brines sourced from the oil and gas industry that include many contaminants [1]. Further work to provide cost estimates and energy consumption of pretreatment will be critical to fully assessing the feasibility of the OARO process.

Finally, we make several simplifying assumptions in our analysis that require further investigation. First, we simplify the OARO model by assuming 100% salt rejection. In reality, salt will diffuse across the membrane and the salt flux will vary for each module in the OARO process. The resulting non-steady state conditions will lead to salt accumulation or depletion within the sweep cycles and will require the addition of a purge stream and/or input of a saline solution for sweep TDS and volume adjustment. Other non-steady state processes, e.g.

variable feed quality and membrane scaling and fouling, were also not assessed. Finally, we assume the membrane properties from experiments with relatively low concentrations and applied hydraulic pressure are applicable for the OARO process [19]. There is significant need for experimental work on the performance of membranes in the high salinity and high pressure operating conditions associated with the OARO process to compliment the modeling work performed in this study. Preliminary experimental work for OARO conditions have recently been reported by Arena et al. [33].

5. Conclusions

The dewatering of high salinity brines is costly due to the high energy demand or low recovery of existing treatment technologies. In this work, we introduce the OARO process and provide first order estimates of physically feasible operating conditions and performance metrics, such as recovery and energy consumption. We observe that the OARO process can obtain reasonable recoveries for reduced or comparable energy consumption as the MVC process, the dominant high salinity brine treatment technology. Future work to determine the feasibility of the OARO process will need to address the implications of our simplifying assumptions, consider the pretreatment requirements for long-term operation, and estimate the cost-competitiveness of this technology.

Disclaimer

This manuscript was prepared as an account of work sponsored by an agency of the United States Government. Neither the United States Government nor any agency thereof, nor any of their employees, makes any warranty, express or implied, or assumes any legal liability or responsibility for the accuracy, completeness, or usefulness of any information, apparatus, product, or process disclosed, or represents that its use would not infringe privately owned rights. Reference therein to any specific commercial product, process, or service by trade name, trademark, manufacturer, or otherwise does not necessarily constitute or imply its endorsement, recommendation, or favoring by the United States Government or any agency thereof. The views and opinions of authors expressed therein do not necessarily state or reflect those of the United States Government or any agency thereof.

Acknowledgements

This work was completed as part of National Energy Technology Laboratory (NETL) research for the U.S. Department of Energy's (DOE) Fossil Energy (FE) program and NSF CBET-1554117 and CBET-1215845. Support for T.V.B. and J.T.A. was provided by appointment to the National Energy Technology Laboratory Research Participation Program, sponsored by the U.S. Department of Energy and administered by the Oak Ridge Institute for Science and Education. T.V.B. was also supported by the ARCS Foundation Fellowship.

Appendix A. Supplementary data

Supplementary data includes the: 1) osmotic pressure calculation, 2) discrete element model for a single OARO module, 3) multi-module model for the OARO process, 4) base case concentration profile, 5) salt rejection, 6) pressure drop. Supplementary data associated with this article can be found in the online version, at http://dx.doi.org/10.1016/j.desal.2017.04.012.

References

[1] D.L. Shaffer, L.H. Arias Chavez, M. Ben-Sasson, S. Romero-Vargas Castrillon, N.Y. Yip, M. Elimelech, Desalination and reuse of high-salinity shale gas produced water: drivers, technologies, and future directions, Environ. Sci. Technol. 47 (17) (2013) 9569.
[2] R. Kaplan, D. Mamrosh, H.H. Salih, S.A. Dastgheib, Assessment of desalination technologies for treatment of a highly saline brine from a potential CO_2 storage site, Desalination 404 (2017) 87.
[3] J.T. Arena, J.C. Jain, C.L. Lopano, J.A. Hakala, T.V. Bartholomew, M.S. Mauter, N.S. Siefert, Management and dewatering of brines extracted from geologic carbon storage sites, Int. J. Greenhouse Gas Control (2017), http://dx.doi.org/10.1016/j.ijggc.2017.03.032.
[4] M. Al-Sahali, H. Ettouney, Developments in thermal desalination processes: design, energy, and costing aspects, Desalination 214 (1) (2007) 227.
[5] A. Alkhudhiri, N. Darwish, N. Hilal, Membrane distillation: a comprehensive review, Desalination 287 (2012) 2.
[6] G.P. Thiel, E.W. Tow, L.D. Banchik, H.W. Chung, V.J.H. Lienhard, Energy consumption in desalinating produced water from shale oil and gas extraction, Desalination 366 (2015) 94.
[7] C. Fritzmann, J. Löwenberg, T. Wintgens, T. Melin, State-of-the-art of reverse osmosis desalination, Desalination 216 (1) (2007) 1.
[8] T.Y. Cath, A.E. Childress, M. Elimelech, Forward osmosis: principles, applications, and recent developments, J. Membr. Sci. 281 (1–2) (2006) 70.
[9] Y. Oh, S. Lee, M. Elimelech, S. Lee, S. Hong, Effect of hydraulic pressure and membrane orientation on water flux and reverse solute flux in pressure assisted osmosis, J. Membr. Sci. 465 (2014) 159.
[10] A. Achilli, A.E. Childress, Pressure retarded osmosis: from the vision of Sidney Loeb to the first prototype installation — review, Desalination 261 (3) (2010) 205.
[11] M. Elimelech, W.A. Phillip, The future of seawater desalination: energy, technology, and the environment, Science 333 (6043) (2011) 712.
[12] Sawyer, J. E.; Lucas, A. L.; Davis, V. M.; Dombek, B. D.; George, E. K., Treatment of waters with multiple contaminants. United States Patent US20140021135 A1, Jan 23, 2014.
[13] Wohlert, C. W., Apparatus and methods for solution processing using reverse osmosis. United States Patent US20130270186 A1, Oct 17, 2013.
[14] R. Lakerveld, J. Kuhn, H.J.M. Kramer, P.J. Jansens, J. Grievink, Membrane assisted crystallization using reverse osmosis: influence of solubility characteristics on experimental application and energy saving potential, Chem. Eng. Sci. 65 (9) (2010) 2689.
[15] S. Loeb, L. Titelman, E. Korngold, J. Freiman, Effect of porous support fabric on osmosis through a Loeb-Sourirajan type asymmetric membrane, J. Membr. Sci. 129 (2) (1997) 243.
[16] J.R. McCutcheon, M. Elimelech, Influence of concentrative and dilutive internal concentration polarization on flux behavior in forward osmosis, J. Membr. Sci. 284 (1–2) (2006) 237.
[17] A. Achilli, T.Y. Cath, A.E. Childress, Selection of inorganic-based draw solutions for forward osmosis applications, J. Membr. Sci. 364 (1–2) (2010) 233.
[18] G. Scatchard, W.J. Hamer, S.E. Wood, Isotonic solutions. I. The chemical potential of water in aqueous solutions of sodium chloride, potassium chloride, sulfuric acid, sucrose, urea and glycerol at 25°1, J. Am. Chem. Soc. 60 (12) (1938) 3061.
[19] Q. She, X. Jin, C.Y. Tang, Osmotic power production from salinity gradient resource by pressure retarded osmosis: effects of operating conditions and reverse solute diffusion, J. Membr. Sci. 401–402 (2012) 262.
[20] E.W. Washburn, International Critical Tables of Numerical Data, Physics, Chemistry and Technology, 1st electronic ed., Knovel, 2003Online version available at http://app.knovel.com/hotlink/toc/id:kpICTNDPC4/international-critical/international-critical.
[21] R.D. Cohen, R.F. Probstein, Colloidal fouling of reverse osmosis membranes, J. Colloid Interface Sci. 114 (1) (1986) 194.
[22] S. Kim, E.M.V. Hoek, Modeling concentration polarization in reverse osmosis processes, Desalination 186 (1) (2005) 111.
[23] J.R. McCutcheon, R.L. McGinnis, M. Elimelech, Desalination by ammonia–carbon dioxide forward osmosis: influence of draw and feed solution concentrations on process performance, J. Membr. Sci. 278 (1–2) (2006) 114.
[24] C.H. Tan, H.Y. Ng, Modified models to predict flux behavior in forward osmosis in consideration of external and internal concentration polarizations, J. Membr. Sci. 324 (1–2) (2008) 209.
[25] J. Schwinge, D.E. Wiley, A.G. Fane, Novel spacer design improves observed flux, J. Membr. Sci. 229 (1–2) (2004) 53.
[26] P. Xie, L.C. Murdoch, D.A. Ladner, Hydrodynamics of sinusoidal spacers for improved reverse osmosis performance, J. Membr. Sci. 453 (2014) 92.
[27] R.L. Maynard, The Merck index: 12th edition 1996, Occup. Environ. Med. 54 (4) (1997) 288.
[28] A. Tiraferri, N.Y. Yip, W.A. Phillip, J.D. Schiffman, M. Elimelech, Relating performance of thin-film composite forward osmosis membranes to support layer formation and structure, J. Membr. Sci. 367 (1–2) (2011) 340.
[29] D.D. Anastasio, J.T. Arena, E.A. Cole, J.R. McCutcheon, Impact of temperature on power density in closed-loop pressure retarded osmosis for grid storage, J. Membr. Sci. 479 (2015) 240.
[30] B.D. Coday, D.M. Heil, P. Xu, T.Y. Cath, Effects of transmembrane hydraulic pressure on performance of forward osmosis membranes, Environ. Sci. Technol. 47 (5) (2013) 2386.
[31] A. Koren, N. Nadav, Mechanical vapour compression to treat oil field produced water, Desalination 98 (1) (1994) 41.
[32] P. Xu, N. Hancock, K. Guerra, T. Cath, J. Drewes, An integrated framework for treatment and management of produced water: technical assessment of produced water treatment technologies, Department of Energy, Research Partnership to Secure Energy for America Project 07122–12, 2009.
[33] J.T. Arena, T.V. Bartholomew, M.S. Mauter, N.S. Siefert, Dewatering of high salinity brines by osmotically assisted reverse osmosis, Proceedings of the 2017 AWWA-AMTA Membrane Technology Conference and Exposition, February 13–17, 2017 (Long Beach, CA, USA).